Spin and energy analyzed photoemission: A feasibility analysis

D. T. Pierce, C. E. Kuyatt, and R. J. Celotta

National Bureau of Standards, Washington, D.C. 20234

(Received 5 April 1979; accepted for publication 15 July 1979)

New scientific opportunities, particularly for investigation of surface magnetism, will be provided by spin and energy analyzed photoemission. Electron-optical conservation laws and phase space concepts are summarized and applied to determine the feasiblity of an experiment consisting of a photoemitter in a magnetic field, a photoelectron energy analyzer and an electron spin analyzer. For the example of photoemission from a Ni crystal using He I resonance radiation and typical parameters for the energy and spin analyzers, a final signal count rate of approximately 220 counts/s is calculated. Ways to increase the count rate by orders of magnitude are described. In particular, a new experimental configuration is suggested which may avoid the large reduction in count rate caused by the magnetic field.

INTRODUCTION

Over the past 15 years, a great deal of knowledge about the electronic structure of solids and surfaces has been derived from photoemission measurements.[1] The simplest photoemission measurement is that of the quantum yield of electrons per photon at each photon energy. The yield measurement is energy integrated in the following sense: all possible transitions at a given photon energy between states separated by that energy contribute to the photocurrent if the final state is above the vacuum level. If, additionally, the kinetic energy of the photoemitted electrons is measured, one can obtain an energy distribution curve (EDC), so that the initial and final state energies of the electron are known (with possible corrections for relaxation). The measurement of the angle of emission in addition to the kinetic energy provides information on the origin of the electron in momentum space.

The degree of spin polarization $P = (N\uparrow - N\downarrow)/(N\uparrow + N\downarrow)$, where $N\uparrow, N\downarrow$ are, respectively, the number of electrons parallel or antiparallel to a quantization direction, is not usually measured in photoemission experiments. The photoelectrons may be polarized, for example, if they are emitted from a ferromagnet in which the domains have been aligned by the application of an external magnetic field. In nonmagnetic materials, photoelectrons may be polarized when excited from spin-orbit-split bands by circularly polarized light. Other causes of spin-polarized photoemission from nonmagnetic surfaces[2] and from gases have been proposed.[3]

The polarization of photoemitted electrons has only been determined to date in an experiment analogous to a quantum yield measurement; that is, the polarization of the total photocurrent is measured as a function of photon energy, $P(\hbar\omega)$. Energy and spin analysis of photoelectrons have not yet been combined. Even so, considerable information has been obtained about the energy location of polarized electron states by measurement of $P(\hbar\omega)$ near photothresholds.[4,5]

Just as most of our knowledge from photoemission measurements has come from energy analysis of the photoelectrons rather than from yield measurements, we expect to learn much more if we can add energy analysis to spin-polarized photoemission measurements. Then polarized electronic states lying deeper in energy can be detected by excitation at higher photon energy. In contrast, yield type measurements are confined to photon energies near threshold, because at higher photon energies information is obscured by the energy integration of many transitions. With energy analysis the initial and final states of the photoelectron will be known. Since measurements will not be limited to threshold, the photon energy can be chosen in the range of intense light sources (such as resonance lamps or monochromatized synchrotron radiation). The photon energy can be varied to change the final state corresponding to a given initial state and to study matrix element effects. It can be chosen so that the photoelectrons have a short mean-free path for inelastic scattering causing the measurement to be very surface sensitive, or it can be chosen so that bulk characteristics are emphasized.

The scientific opportunities for spin and energy analyzed photoemission are numerous and varied. Energy analysis will allow an accurate determination of the energies of magnetic levels in solids. In nonmagnetic materials, information on the spin properties of the wavefunctions can be obtained.[6,7] By adjusting the photon energy to enhance surface sensitivity, energy analyzed spin-polarized photoemission will provide a measure of the surface magnetization. Measurements as a function of temperature will permit studies of an approximately two-dimensional critical phenomenon. Measurements of P when gases are adsorbed on a magnetic surface will give information on the role of local moments in chemisorption.

The elements of an energy analyzed spin-polarized photoemission experiment will be presented in Sec. I. The experiment is seen to be difficult because an electron beam which originated at a photocathode in a magnetic field has low electron-optical brightness when

 0034-6748/79/111467-07$00.60

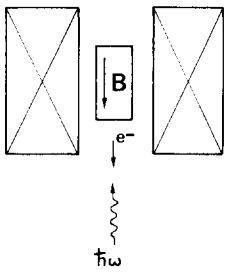

FIG. 1. The photocathode configuration employed in successful spin-polarized photoemission measurements to date. A coil produces a magnetic field perpendicular to the sample surface and colinear with the electron beam.

it is outside the field, and because the spin detectors are inefficient. Because of these difficulties, it is essential to consider carefully the electron-optical characteristics of each stage of the experiment. In Sec. II, some background on electron-optical conservation laws is given and each part of the experiment, the photocathode, the energy analyzer, and the spin detector, is analyzed separately. In Sec. III we make quantitative estimates for an energy analyzed spin-polarized photoemission measurement of Ni. Estimates can be made of the maximum signal to be expected, assuming other aspects of the experiment, such as alignment, are optimized. Ways to improve the experiment, including a novel configuration, will be discussed.

I. THE EXPERIMENT AND THE DIFFICULTIES

Successful spin-polarized photoemission measurements[4,5] to date have been accomplished using the photocathode configuration shown in Fig. 1. The magnetic field axis, the electron beam axis and the light direction are colinear and normal to the sample surface. The spin polarization is longitudinal, that is, colinear with the electron beam. The possibility of using an alternate configuration will be discussed in Sec. III. The spin is analyzed by a Mott detector.[8] The transverse polarization required for the Mott detector may be obtained by a 90° electrostatic deflection of the beam or by a spin rotation in crossed electric and magnetic fields as in a Wien filter. Since the transverse polarization can be obtained without beam loss, we shall not discuss such devices further. A detailed schematic of a spin-polarized photoemission apparatus can be found in Ref. 4.

The two major difficulties of the experiment are caused by the magnetic field normal to the sample surface and by the inefficiency of the Mott detector. The magnetic field is required to align the domains of a magnetic sample. Even in the case of a permanent magnet requiring no applied field, the field inside and outside is the same, $B_i = B_o$, since the normal component of B is continuous across the surface. Typically in an experiment B is of the order of the saturation magnetizations, since then the polarization is maximum.

The magnetic field at the cathode causes the beam to have low electron-optical brightness outside the magnetic field. Electrons emitted off axis in the magnetic field have an angular momentum $\mathbf{r} \times (m\mathbf{v} - e\mathbf{A})$, where m is the electron mass, $\mathbf{v}$ its velocity, $-e$ its charge, and $\mathbf{A}$ the magnetic vector potential. In a cylindrically symmetric system with coordinates r, θ, z, the axial component of the angular momentum, or equivalently the component of canonical momentum P_θ conjugate to the cyclic coordinate θ, is conserved,

$$P_\theta = mr^2\dot{\theta} - erA_\theta(r,z) = \text{constant}. \quad (1)$$

The canonical angular momentum of off-axis electrons, $r \neq 0$, in the longitudinal magnetic field corresponding to the vector potential A_θ, goes into kinetic angular momentum and hence skew trajectories in regions of reduced magnetic field. Eq. (1) is the basis of Busch's theorem which will be discussed in Sec. II.

Spin analysis is traditionally carried out using a Mott detector. In a Mott detector, energetic electrons (~100 keV) are scattered from heavy nuclei, such as gold. The interaction of the electron's spin with its own orbital angular momentum as it scatters gives rise to a left-right asymmetry in the numbers N_l, N_r of electrons scattered into the detectors depending on whether the polarization P is parallel or antiparallel to the normal to the scattering plane:

$$N_l = (N/2)(1 + SP), \quad N_r = (N/2)(1 - SP). \quad (2)$$

For scattering from Au, thin foils must be used to avoid multiple scattering. Most of the N_0 incident electrons go right through this foil and only a small number $N = N_l + N_r$ are backscattered at 120° into the detectors. Depending on detector area, N/N_0 typically ranges from 10^{-3} to 10^{-5}. The size of the asymmetry depends on S, which for Au foils typically used is ~0.25. The statistical uncertainty (standard deviation) in the polarization measurement is given by[8]

$$\Delta P \simeq \sqrt{1/NS^2}. \quad (3)$$

Because $S < 1$, a greater count rate is required to reach a given precision. To compensate for losses in the spin analysis, N_0 would have to be greater by a factor of at least 10^4.

Clearly, both the photocathode in a magnetic field and the spin analysis are sources of difficulty in the experiment. In the case of spin polarized photoemission from nonmagnetic materials no magnetic field is required. With only the losses due to spin analysis the experiment is easier.

II. ANALYSIS

A. Electron-optical conservation laws

By applying phase space concepts in the analysis of the experiment we can estimate its feasibility without performing any detailed calculations of the electron trajectories. If electrons are represented in phase space by coordinates x, y, z and conjugate momenta P_x, P_y, P_z, then Liouville's theorem states that the volume element at point a is the same as that at a later time when the beam has propagated to another point b,

$$dx^a dy^a dz^a dP_x{}^a dP_y{}^a dP_z{}^a = dx^b dy^b dz^b dP_x{}^b dP_y{}^b dP_z{}^b. \quad (4)$$

The points in phase space behave like an incompressible fluid and the density of particles in phase space is constant for a Hamiltonian system according to Liouville's theorem. The system we are considering, of electrons moving in macroscopic electric and magnetic fields, is Hamiltonian. An example of a non-Hamiltonian system is one in which the radiative damping of an accelerated charge needs to be considered.[9]

The envelope of an electron beam emitted from a photocathode in a magnetic field encloses a certain volume in phase space. The energy analyzer and spin detector accept a limited volume of phase space. If the phase space occupied by the emitted beam is greater than that accepted by one of the other components, there will be electrons lost.

In our problem we are concerned with the effect (focusing, deflection, etc.) of electron-optical components on the motions of particles in x and y directions which are locally perpendicular to the (not necessarily straight) beam path along z. If we consider a nearly monoenergetic beam of particles and ignore aberrations and other coupling of the x and y motions to the z motion, we can work in a phase space of lower dimension,[9] where the volume element is $dxdydP_xdP_y$. The canonical momentum is $\mathbf{P} = p\boldsymbol{\xi} - e\mathbf{A}$, where p is the electron momentum in a direction given by the direction cosines ξ_x, ξ_y, and ξ_z. In a paraxial ray approximation the velocity in the z direction is unaffected by small transverse displacements. In the absence of a magnetic field, $dP_x = dp_x = p_z d\xi_x$.

The conserved quantity $dxdydP_xdP_y$ in this four-dimensional space may therefore be written,

$$EdAd\Omega = \text{constant}, \tag{5}$$

where $E = p^2/2m$ is the beam energy, $dA = dxdy$ is the differential area, and $d\Omega = d\xi_x d\xi_y$ is the differential solid angle of the beam at some cross section. Although Eq. (5) is more general,[10] it is usually applied to the paraxial beam situation we are considering; in this case Eq. (5) can be integrated to give an equation for the conservation of the phase space product,

$$E_1A_1\Omega_1 = E_2A_2\Omega_2, \tag{6}$$

for any two cross sections 1 and 2 along the beam. Related to the phase space product is the electron-optical brightness defined as[11] $\mathcal{B} = dI/dAd\Omega$, where dI is the differential current through a differential area dA and $d\Omega$ is the solid angle subtended by the electron beam at dA. When the current is conserved Eq. (5) gives $\mathcal{B}/E$ = constant.

There are some integral invariants which characterize certain properties of an electron beam and remain constant during the motion. These are useful for calculating the effective phase space product when magnetic fields are present. We consider a set of electron trajectories passing through a surface S_1 bounded by the curve C_1 and then through surface S_2 bounded by C_2. The Lagrange integral invariant is[12,13]

$$\int_{S_1} (\nabla \times \mathbf{P})\cdot d\mathbf{S} = \int_{S_2} (\nabla \times \mathbf{P})\cdot d\mathbf{S} \tag{7}$$

In hydrodynamic terms, this equation expresses the conservation of vorticity $\nabla \times \mathbf{P}$. The line integral form of Lagrange's invariant is called Poincaré's invariant and is expressed as

$$\oint_{C_1} \mathbf{P}\cdot d\mathbf{l} = \oint_{C_2} \mathbf{P}\cdot d\mathbf{l}. \tag{8}$$

Equation (8) will be applied in the next section to the analysis of the photocathode in a magnetic field. Further discussion and a proof of these invariants can be found in Refs. 12 and 13.

A generalized form of Busch's theorem is obtained from Eq. (8), using $\mathbf{P} = \mathbf{p} - e\mathbf{A}$ and Stokes' theorem,

$$\oint_{C_1} \mathbf{p}\cdot d\mathbf{l} - \oint_{C_2} \mathbf{p}\cdot d\mathbf{l} = e\int_{S_1} \mathbf{B}\cdot d\mathbf{S} - e\int_{S_2} \mathbf{B}\cdot d\mathbf{S}. \tag{9}$$

In an axially symmetric system, if the two closed curves C_1 and C_2 are circles of radii r_1 and r_2 enclosing surfaces S_1 and S_2 with planes perpendicular to the axis, we obtain Busch's theorem

$$r_1^2\dot{\theta}_1 - r_2^2\dot{\theta}_2 = (e/2m)(r_1^2B_{n1} - r_2^2B_{n2}), \tag{10}$$

where B_{nj} is the component of B_j normal to surface S_j. The increase in the kinetic angular momentum between two points is proportional to the change in magnetic flux through the beam cross section at the two points. In Eq. (10), $\dot{\theta}$ is the angular velocity of an electron about the axis. Since the magnetic field along the axis is $B_n = 2A_\theta/r$, Eq. (10) is just a statement that the axial component of the canonical angular momentum is conserved. Thus, a beam originating from a finite area at a cathode where $\dot{\theta}_1 = 0$ and $B_{n1} \neq 0$, cannot according to Eq. (10) be focused somewhere else to a point, that is where $r_2 = 0$. More generally, from Eq. (7) if we consider S_1 to be in the cathode surface and the component of $\mathbf{p}$ tangent to the cathode surface is zero,[13]

$$\int_{S_2} (\nabla \times \mathbf{P})\cdot d\mathbf{S} = \int_{S_1} [(\nabla \times \mathbf{p}) - e\mathbf{B}]\cdot d\mathbf{S} = -e\int_{S_1} B_n dS. \tag{11}$$

If B_n at the cathode is zero, $\nabla \times \mathbf{P} = 0$ and hence $\mathbf{P} = \nabla V$, where V is a scalar function of position only. The vector $\mathbf{P}$ forms an irrotational field and the flow is said to be congruent. In this case, Poincaré's invariant vanishes, which is equivalent to saying that a system of rays emanates from a point. Likewise, a given system of rays can only be focused to a point if the Poincaré invariant vanishes. On the other hand, if B_n is nonzero, $\mathbf{P}$ does not form an irrotational field and the flow is said to be noncongruent. We apply these electron-optical concepts to analyze the spin and energy analyzed photoemission experiment, element by element, in the next sections.

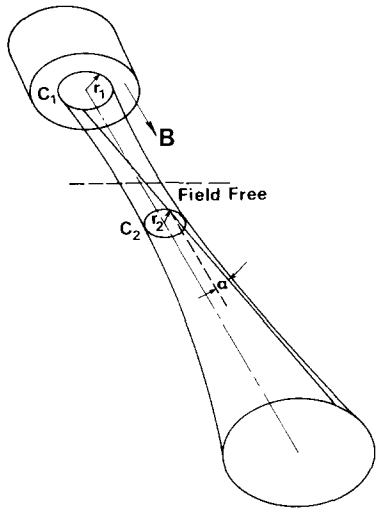

FIG. 2. Diagram for applying the Poincaré invariant to a photocathode in a magnetic field. The illuminated area of the sample is bounded by the circle C_1 of radius r_1 and is located in a magnetic field B_n normal to the surface. The minimum diameter of the beam outside the B field is r_2.

B. The photocathode

The Poincaré invariant, Eq. (8), can be applied at a photocathode where $B_n \neq 0$ to determine the smallest area solid angle product which can be achieved by the beam focused outside the magnetic field. We consider an axially symmetric tube of rays emanating from the illuminated area of the cathode surface enclosed by a circle C_1 of radius r_1. The initial energy of the electrons is neglected and there is a magnetic field B_n. Using Poincaré's invariant at the cathode we have

$$\oint_{C_1} P_\theta d\theta = 2\pi r_1 e A_\theta = \pi r_1^2 e B_n. \tag{12}$$

The envelope of the rays is a hyperboloid of revolution[10] as in Fig. 2. Now we consider the Poincaré integral at the minimum radius r_2, where the half-angle of the cone formed by the asymptotic ray of the envelope is α,

$$\oint_{C_2} P_\theta d\theta = 2\pi p_2 r_2 \sin\alpha. \tag{13}$$

For rays near the axis, $\sin\alpha \approx \alpha$ and equating Eqs. (12) and (13) we can write a generalized emittance

$$\epsilon = r_2\alpha = \tfrac{1}{2} e r_1^2 B_n / p_2. \tag{14}$$

Noting that the tangential velocity $r_2\dot{\theta}_2 = v\sin\alpha \approx v\alpha$, a similar result can be obtained from Busch's theorem. The emittance in a magnetic field has also been considered by Hughes *et al.*[14] Because $A\Omega = \pi^2\epsilon^2$, we find for our phase space product for the envelope of an electron beam emitted at zero energy from a photocathode in a magnetic field,

$$\begin{aligned} EA\Omega &= (\pi^2 e^2/8m) r_1^4 B_n^2 \\ &= 2.17 \times 10^{-3} r_1^4 B_n^2 \text{ mm}^2\cdot\text{sr}\cdot\text{eV}, \end{aligned} \tag{15}$$

where the radius is expressed in millimeters and the magnetic field in gauss.

C. The energy analyzer

We next wish to determine the phase space product $EA\Omega$ that the energy analyzer can accept. An important property of an energy analyzer is the resolving power $\rho = E_0/\Delta E_{1/2}$, where E_0 is the central energy of the pass-band of the electrons in the analyzer, and $\Delta E_{1/2}$ is the full width at half-maximum of the energy spread of the analyzed beam. The figure of merit for an energy analyzer is[15]

$$M = \rho A_0\Omega_0 = E_0 A_0\Omega_0/\Delta E_{1/2}. \tag{16}$$

This allows the comparison of analyzers which operate at different energies E_0. There is a trade-off between the acceptance $(A_0\Omega_0)$ of an analyzer and the resolving power. Since the acceptance of analyzers always increases faster than ρ decreases, M is maximized when the analyzer is operated at the lowest practical value of ρ.

The figure of merit of an analyzer increases with its size. For a 180° spherical analyzer

$$M = 20R^2\alpha^4 \text{mm}^2\cdot\text{sr}, \tag{17}$$

where the mean radius of the beam path R is in millimeters and the acceptance cone half-angle α is in radians. There are similar relations for other types of analyzers showing that, in general, M increases as the square of a characteristic dimension. To get a feeling for the numbers, a spherical analyzer with 100-mm mean radius and an acceptance angle α of 0.1 rad has $M = 20$ mm$^2\cdot$sr. This, for example, is the same M as a commercial single pass cylindrical mirror analyzer used on a scanning Auger microscope.

D. The spin analyzer

There are several factors to be considered in determining the effect of the spin analyzer on the signal to be measured. First, the $EA\Omega$ product tells us what fraction of the electrons are accepted by the device. Secondly, in the case of the scattering-type spin analyzers we will consider, there is some fraction N/N_0 of the incident electrons N_0 which reach the detectors and there is a scattering asymmetry S.

For the Mott detector which was introduced in Sec. I, we can get an idea of $EA\Omega$ from some typical numbers. A typical Mott detector might focus the beam to a 2-mm-diam spot at 100 keV with a cone half-angle of 1°. This gives $EA\Omega \approx 300$ mm$^2\cdot$sr$\cdot$eV. The high final energy, which is perhaps experimentally inconvenient, increases greatly the phase space accepted by the Mott analyzer. The signal losses caused by the Mott analyzer are due to the factor S^2N/N_0. A typical Mott detector has $S^2N/N_0 = 6.3 \times 10^{-6}$ ($S = 0.25$, $N/N_0 = 10^{-4}$). S^2N/N_0 is the figure of merit for a Mott detector. However, if not all of the electron beam is accepted by the Mott detector, the figure of merit is reduced by $(EA\Omega)_d/(EA\Omega)_i$, where d and i refer to the detector and incident beam phase space, respectively.

There is the possibility of increasing S^2N/N_0 by exploiting spin-polarization effects in polarized low-energy

electron diffraction (PLEED) from high atomic number single crystals.[16] The first prototype of such a detector operates[17] at 105 eV and has $S^2N/N_0 = 8.6 \times 10^{-5}$ ($S = 0.28, N/N_0 = 1.1 \times 10^{-3}$). The angular acceptance is approximately a 0.5° cone half-angle with a 2-mm-diam limiting aperture,[18] which gives $EA\Omega = 0.08$ mm²·sr·eV. While at this time this type of detector is in the experimental stage, it has the advantage of being a small, bakeable ultrahigh vacuum device which makes it attractive for spin and energy analyzed photoemission.

III. DISCUSSION

The above phase space consideration of the energy and spin analyzed photoemission experiment are sufficient to estimate the count rates to be expected for a given experiment and hence the expected precision ΔP in the polarization for a given measurement time. We illustrate this by carrying through the analysis for a Ni sample using a He I resonance lamp at 21.2 eV. Ways to improve the count rate will then be discussed.

A. Ni example

We consider a Ni crystal illuminated by a He discharge lamp at 21.2 eV. The most energetic electrons have an energy of approximately 16 eV. A typical total emitted photocurrent is 10^{-9} A. This corresponds to a light flux of 2×10^{11} photons/s and a quantum yield of 3%. We select an energy resolution of 0.2 eV and then have 80 0.2-eV channels in the distribution of emitted electrons which have on the average 8×10^7 electrons/s in each channel. We wish to follow these electrons and determine the final signal count rate.

The saturation magnetization in Ni is about 6 kG. If the crystal area illuminated by the resonance lamp is 1 mm diam, we have from Eq. (15), $EA\Omega = 4880$ mm²·sr·eV. For a spherical energy analyzer such as that discussed in Sec. II C, with $M = 20$ mm²·sr, the phase space for $\Delta E_{1/2} = 0.2$ eV is $M\Delta E_{1/2} = 4$ mm²·sr·eV. The large disparity between the phase space product of the photocathode and the energy analyzer means a large loss in the electron beam. The loss is determined by calculating the largest ring of radius r illuminated on the cathode which yields a beam envelope with $EA\Omega$ that can be accepted by the energy analyzer. All annular-shaped areas of smaller radius will have smaller $EA\Omega$. The loss is not as large as might appear at first glance, since the $EA\Omega$ for a cathode in a magnetic field decreases as r^4 while the intensity is proportional to the area or r^2. In our Ni example, only the central region of the Ni crystal, 0.17 mm diam, yields photocurrent which can be accepted by the energy analyzer, corresponding to a factor of 35 intensity loss.

In Eq. (15) the initial energies of the electrons have been neglected. Electrons emitted from near the Fermi level have an energy near 16 eV. In the absence of a magnetic field and for isotropic emission, the effective area-solid angle product is $A\Omega = \pi A$. For a 0.17-mm-diam emitting area $EA\Omega = 1.1$ mm²·sr·eV, approximately one-quarter that of the photocathode in a magnetic field. Any angular dependence of the emission is obscured by the skew trajectories caused by the magnetic field. The magnetic field does not cause a problem in a field emission measurement because of the small emitting area. It has been possible to combine spin analysis and energy analysis (using a retarding field rather than a dispersive energy analyzer) in a field emission measurement of EuS.[19]

At the Mott detector we have the loss due to the factor N/N_0. Taking a typical value $N/N_0 = 10^{-4}$, coupled with the factor of 35 loss at the energy analyzer, the average count rate is reduced from 7.8×10^7 counts/s to 223 counts/s. Using Eq. (3) with $S = 0.25$ we find $\Delta P = 2\%$ for a 180-s integration time. For the prototype PLEED detector discussed above, the count rate would be 49 counts/s, and a precision of 2% requires an integration time of ~650 s. While these are reasonable signals, they are marginal for a surface-sensitive experiment (e.g., Ni at $\hbar\omega = 21.2$ eV) where surface contamination can be a problem. Also, for other samples, such as Fe or Co which require higher magnetic fields, the losses are more severe. Some ways the signal might be increased are discussed in the next section.

B. Improving the count rate

The most obvious way to improve the count rate is to start with more electrons. High-brightness storage rings with efficient monochromators provide intense sources of synchrotron radiation. As seen above, large factors can be won if the incident radiation is focused to a small spot on the sample surface. Suitable resolution can be achieved with a monochromator bandpass of several Å which can provide a larger total number of photons than the narrow He I resonance line. While from Eq. (15) it would also be desirable to reduce B, in the experimental configuration of Fig. 1 there would be a corresponding decrease in P.

The figure of merit of the energy analyzer can be increased, Eq. (17), by making it physically larger. Suitable combinations of lenses can also increase α. An increase in the figure of merit of up to a factor of 10 over the typical value used in the Ni example might be gained by optimizing the energy analyzer.

The figure of merit of the Mott detector S^2N/N_0 can also be increased. S is a parameter of gold and reaches a maximim $S_0 = 0.39$ for a zero-thickness foil and 100-keV electrons. It varies as

$$S = S_0(1 + \alpha d)^{-1}, \tag{18}$$

where $\alpha = 0.0026$ is a constant and d is the thickness.[20] For thin foils, N/N_0 increases linearly with thickness, whereas S decreases approximately linearly with thickness. Therefore one gains in the figure of merit by going to a thinner foil. However, an S greater than 0.3 corresponding to a foil thickness of approximately 100 μg/cm² is impractical. The largest improvements in the Mott detector can be achieved by increasing N/N_0

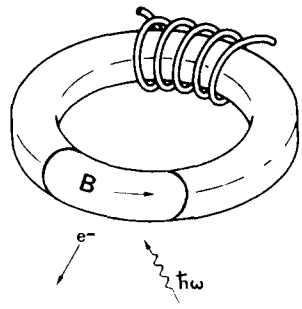

FIG. 3. Suggested configuration with B field in the surface. B outside the surface is very small.

by increasing detector size or number of detectors. The largest N/N_0 reported[21] to date is 1.5×10^{-3} with $S = 0.26$. This represents a figure of merit 16 times greater than the typical value used in the Ni example and gives an idea of what can be achieved by Mott detector optimization.

The PLEED spin detector has great potential for improvement over the prototype described in Sec. II D. PLEED experiments are in progress at NBS to find an optimum material and diffraction configuration. If a condition can be found where S is large and insensitive to angle variations, a large solid angle and beam diameter could be accepted so that $EA\Omega$ could reach 4 mm$^2 \cdot$sr$\cdot$eV with $S^2N/N_0 \approx 10^{-2}$. Further spin detector development is necessary before a definitive comparison of detectors can be made.

C. Proposed experimental configuration

As can be seen from Eq. (11) it is the component of **B** normal to the photocathode surface that causes the trouble. A configuration with **B** in the surface is shown in Fig. 3. The sample to be studied completes the toroidal magnetic circuit. In this case the applied field **H** is continuous across the surface. The B field outside is much smaller than inside. In this geometry only a small H field need be applied to magnetize the sample. In the case of Ni along the easy direction of magnetization [111], only about 50 Oe is required. In favorable cases, the applied field can be removed after the crystal is magnetized.

Such a configuration with **B** parallel to the surface goes against the conventional wisdom.[4] Earlier experiments[22–24] performed using this geometry failed to observe any spin polarization in photoemission from Fe, Co, and Ni. However, this failure is likely attributable to the vacuum conditions in these experiments and failure to minimize stray magnetic fields, particularly those normal to the cathode. Sufficient accelerating potential must be applied to extract the electrons from the emitter when there is a magnetic field parallel to the surface. For example, an electric field of a few hundred V/cm is sufficient to extract the electrons so they are deflected $\lesssim 1$ mm in traveling 1 cm through a magnetic field of the order of 10 G. Note that the spin and magnetic field are colinear so there is no precession, the same as in Fig. 1. It is critical that there be no stray B normal to the surface which would cause a presession of the spin and loss of the spin-polarization information. For example, a 10-eV electron precesses ~0.1 rad/cm in a 1 G field. Because of the high permeability of the toroid material, B_n can be less than 1% of the tangential B, even when the winding on the toroid is concentrated as in Fig. 3.[25] If the stray field normal to the photocathode surface is sufficiently small, the magnetic field at the cathode is no longer a problem. The count rate in our Ni example would be increased by a factor of 35 to 7.8×10^3 counts/s and the integration time for a 2% uncertainty reduced to ~5 s. The experiment can then be treated as a conventional photoemission experiment with the difference in count rate being just due to losses at the spin detector. Angular resolution of the emitted electrons is also possible in this configuration.

IV. DISCUSSION

Using phase space concepts and electron optical conservation laws it has been possible to determine the feasibility of the energy and spin analyzed photoemission experiment, for the specific example of a Ni crystal and a He I resonance lamp. The estimated final count rate of ~220 counts/s provides an uncertainty in the polarization ΔP of 2% for a 180-s integration time. Although typical parameters were used in the estimate, each part of the experiment—the photoemission, the energy analyzer, and the spin analyzer—can be further optimized. An intense, well-focused light source, a large energy analyzer with large acceptance angle, and a Mott analyzer with a large detector area can greatly improve the count rate in the traditional experimental configuration. Each improvement is important, facilitates surface-sensitive measurements, and can compensate for possible losses due to other factors such as imperfect alignment. An experimental configuration has been proposed which will reduce the problem associated with the magnetic field at the sample surface, reduce the integration time for a 2% uncertainty to 5 s without other improvements, and allow angle analysis. In short, the experiment looks promising. Spin, angle and energy analyzed photoemission is an exciting new experimental technique and will be a powerful way to investigate bulk and surface magnetism.

Note added in proof: The proposed new experimental configuration has been successfully used in a polarized low energy diffraction (PLEED) experiment on ferromagnetic Ni(110) at energies as low as 20 eV. [R. J. Celotta, D. T. Pierce, G.-C. Wang, S. D. Bader, and G. P. Felcher, Phys. Rev. Lett. **43**, 728 (1979).]

ACKNOWLEDGMENTS

We wish to thank A. Galejs and B. Dunlap for helpful discussions. We are grateful to M. Campagna, M. Landolt, and W. Eib whose inquiries about the electron optics of spin and energy analyzed photoemission experiments in magnetic fields stimulated the presenta-

tion of this work. Supported in part by the Office of Naval Research.

[1] B. Feuerbacher, B. Fitton, and R. F. Willis, *Photoemission and the Electronic Properties of Surfaces* (Wiley, New York, 1978).
[2] R. Feder, Solid State Commun. **28,** 27 (1978).
[3] U. Heinzmann, G. Schönhense, and J. Kessler, Phys. Rev. Lett. **42,** 1603 (1979).
[4] M. Campagna, D. T. Pierce, F. Meier, K. Sattler, and H. C. Siegmann, Adv. in Electron. Electron Phys. **41,** 113 (1976).
[5] S. F. Alvarado, W. Eib, F. Meier, H. C. Siegmann, and P. Zürcher, in *Photoemission and the Electronics Properties of Surfaces*, edited by B. Feuerbacher *et al.* (Wiley, New York, 1978), p. 437.
[6] D. T. Pierce and F. Meier, Phys. Rev. B **13,** 5484 (1976).
[7] P. Zürcher, F. Meier, and N. E. Christensen, Phys. Rev. Lett. **43,** 54 (1979).
[8] J. Kessler, *Polarized Electrons* (Springer-Verlag, New York, 1976).
[9] D. L. Judd, *Annual Review of Nuclear Science*, Vol. 8 edited by E. Sigre (Annual Reviews, Palo Alto, 1958) p. 181.
[10] P. A. Sturrock, *Static and Dynamic Electron Optics* (Cambridge U. P., New York, 1955), Chap. 2.
[11] C. E. Kuyatt and J. A. Simpson, Rev. Sci. Instrum. **38,** 103 (1967).
[12] D. Gabor, Proc. I.R.E. **33,** 792 (1945).
[13] P. T. Kirstein, G. S. Kino, and W. E. Waters, *Space Charge Flow* (McGraw-Hill, New York, 1967), Sec. I. 3.
[14] V. W. Hughes, R. L. Long, Jr., M. S. Lubell, M. Posner, and W. Raith, Phys. Rev. A **5,** 195 (1972).
[15] C. E. Kuyatt (to be published).
[16] D. T. Pierce, R. J. Celotta, W. N. Unertl, *Proc. of the 7th Intl. Vac. Congress and the 3rd Intl. Conf. on Solid Surfaces*, Vienna, 1977, p. 1297.
[17] J. Kirschner and R. Feder, Phys. Rev. Lett. **42,** 1008 (1979).
[18] J. Kirschner (private communication).
[19] E. Kisker, G. Baum, A. H. Mahan, W. Raith and B. Reihl, Phys. Rev. B **18** 2256 (1978).
[20] E. Garwin, F. Meier, D. T. Pierce, K. Sattler, and H. C. Siegmann, Nucl. Instrum. Methods **120,** 483 (1974).
[21] U. Heinzmann, H. Heuer, and J. Kessler, Phys. Rev. Lett. **34,** 441 (1975).
[22] H. A. Fowler and L. Marton, Bull. Am. Phys. Soc. **4,** 235 (1959).
[23] R. L. Long, Jr., V. W. Hughes, J. S. Greenberg, I. Ames, and R. L. Christensen, Phys. Rev. **138,** A1630 (1965).
[24] A. B. Baganov and D. B. Diatroptov, Sov. Phys. JETP **27,** 713 (1968).
[25] D. R. Corson and P. Lorrain, *Introduction to Electromagnetic Fields and Waves* (Freeman, San Francisco, 1962), p. 292.